Patchy Nanocapsules of Poly(vinylferrocene)-Based Block Copolymers for Redox-Responsive Release

Roland H. Staff,[†] Markus Gallei,[‡,*] Markus Mazurowski,[‡] Matthias Rehahn,[‡] Rüdiger Berger,[†] Katharina Landfester,[†] and Daniel Crespy[†,*]

[†]Max Planck Institute for Polymer Research, Ackermannweg 10, 55128 Mainz, Germany and [‡]Ernst-Berl Institute for Chemical Engineering and Macromolecular Science, Darmstadt University of Technology, Petersenstrasse 22, 64287 Darmstadt, Germany

ABSTRACT Nanocapsules composed of a poly(vinylferrocene)-*block*-poly(methyl methacrylate) shell and a hydrophobic liquid core are prepared in water. The nanocapsule shells display a patchy structure with poly(vinylferrocene) patches with sizes of 25 ± 3 nm surrounded by poly(methyl methacrylate). The functional nanopatches can be selectively oxidized, thereby influencing the colloidal morphology and introducing polar domains in the nanocapsule shell. The hydrophobic to hydrophilic transition in the redox-responsive nanopatches can be advantageously used to release a hydrophobic payload encapsulated in the core by an oxidation reaction.

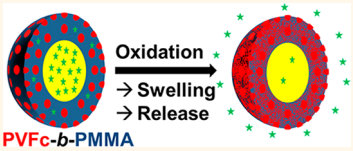

KEYWORDS: ferrocene · nanocapsules · patchy · redox-responsive · stimuli-responsive

Oxidations and reductions are important reactions occurring in nature.[1,2] A balanced concentration of redox-active species is necessary in plants and animals since these species can be both beneficial, as for redox signaling,[3] and detrimental, as for oxidative stress in cells.[4,5] The disulfide bond can be cleaved by a reduction, and this reversible reaction plays an important role in the conformation, and therefore the activity, of many proteins. This principle was transferred to synthetic materials with disulfide bonds to yield mesoporous silica,[6,7] hollow particles,[8] or liposomes[9] with redox-responsive release. Other approaches for the preparation of redox-responsive materials based on quinone derivatives,[10] supramolecular chemistry,[11] or the transition from sulfides to sulfoxides and sulfones upon oxidation in polymers were also proposed.[12]

Another interesting redox couple is the ferrocenium/ferrocene pair, as it was already well explored for biosensor applications[13−18] and for redox-responsive self-healing in host−guest polymers.[19] Furthermore, ferrocene-containing polymers attracted a lot of attention in the past decade due to their promising combination of redox, mechanical, semiconductive, photophysical, optoelectronic, and magnetic properties.[20−26] Since Manners' discovery of the living ring-opening polymerization of *ansa*-metallocenophanes[27−29] leading to polymers with ferrocenes in the polymer main chain, and the improved anionic polymerization of vinylferrocene and ferrocenyl methyl methacrylates leading to laterally bonded ferrocene polymers,[30,31] well-defined and high molecular weight ferrocene polymers with interesting properties were synthesized.

However, up to now there is no report on functional nanocapsules (core−shell nanoparticles with liquid core) based on a material with ferrocene units. Nanocapsules (NCs) have the advantage of keeping their structural integrity compared to non-cross-linked micelles that are subjected to unimer/micelle equilibrium. Miniemulsion droplets are typically used as templates for the preparation of nanocapsules either of organic[32,33] or inorganic nature.[34] Although the miniemulsion systems can be adapted to many different polymerization types,[35] it is sometimes preferable to avoid reactions in the miniemulsion droplets because the product can be difficult to purify without damaging the structural integrity or reducing the stability of the colloids. Different dispersion processes that do not involve reactions were extensively reviewed by Texter for preparing organic submicrometer particles.[36] Building the dispersed phase of a miniemulsion with a solution of polymer

* Address correspondence to crespy@mpip-mainz.mpg.de.

Received for review July 15, 2012 and accepted September 28, 2012.

Published online September 28, 2012
10.1021/nn3031589

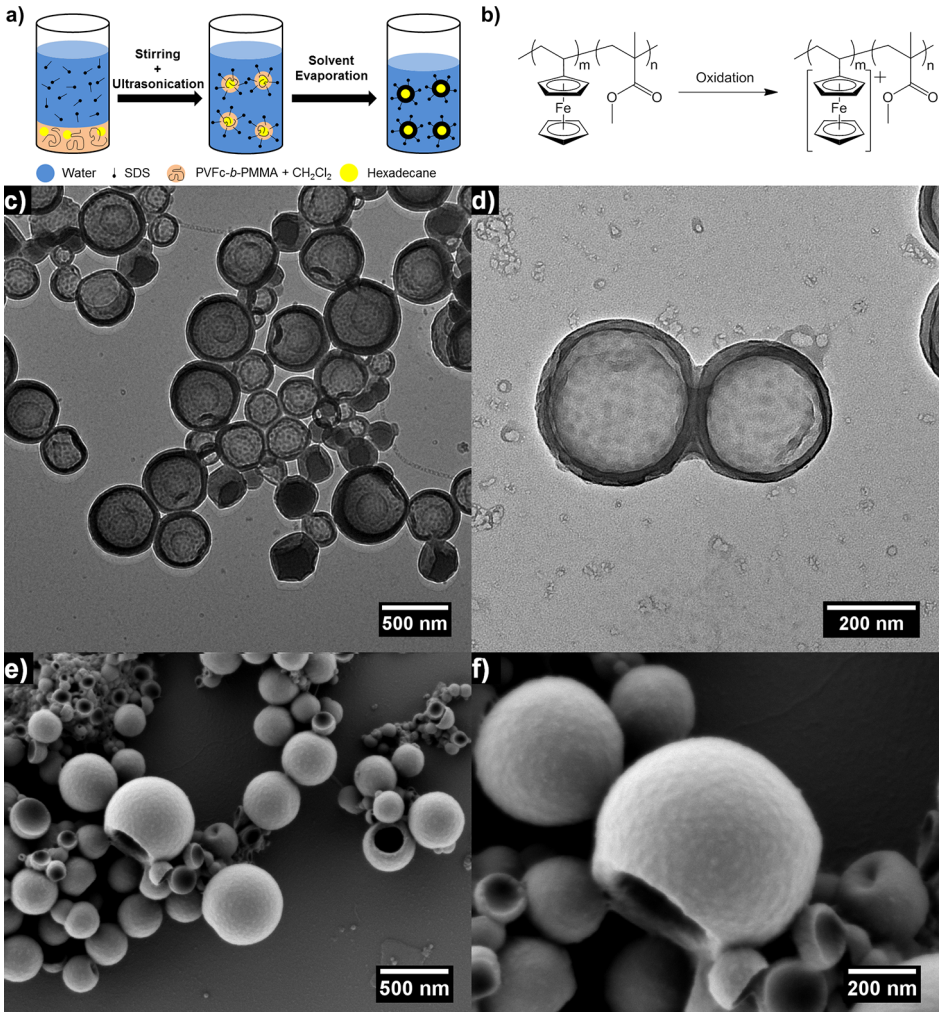

Figure 1. Schematics for the preparation of the NCs (a) with PVFc-*b*-PMMA, a polymer which can be subsequently oxidized (b). TEM micrographs (c, d) and SEM micrographs (e, f) of the dialyzed NCs. In TEM, the microphase separation is evidenced by the presence of dark domains (PVFc block) in the PMMA surrounding matrix.

instead of a liquid monomer avoids possible degradation of the nanoparticles' structure upon their purification when the solvent in the dispersed phase can be subsequently evaporated after the preparation of the nanodroplets. Thus, it was possible to fabricate unconventional polymer dispersions with semiconducting,[37] polyamide 6,[38] syndiotactic or isotactic polystyrene,[39] and polystyrene-*block*-poly(methyl methacrylate) nanoparticles (NPs).[40] A valuable redox-responsive nanoobject such as a nanocapsule should also allow the triggered diffusion of substances encapsulated in its core upon a redox stimulus. This represents one the most challenging tasks in colloid science when the triggered release must be coupled with the maintenance of the structural integrity and colloidal stability of the nanocontainers. One promising answer to overcome this issue is the preparation of patchy nanocapsules with responsive patches located in the nanocapsule shell. Indeed, patches present in the capsule shells can act as channels for the diffusion of substances present in the core while keeping the structural integrity of the shell. Whereas patchy nanocapsules from block copolymers were reported in the literature, they presented neither functionality nor responsive behavior.[40] We aimed here at preparing patchy NCs from redox-responsive PVFc-*b*-PMMA block copolymers and monitoring the release of guest-encapsulated substances from their cores upon selective oxidation of the nanopatches.

RESULTS AND DISCUSSION

Preparation of the Patchy Colloids. For the preparation of NCs, the redox-responsive PVFc-*b*-PMMA block copolymer (see Figure 1a) was dissolved in dichloromethane containing a small amount of hexadecane (a nonsolvent for the copolymer) and mixed with an aqueous solution of SDS by stirring and ultrasonication. After evaporation of the dichloromethane, opaque yellowish dispersions of NCs were obtained. These dispersions were later used for the oxidation experiments (see Figure 1b). The average diameter of the NCs was about 236 $\pm$ 110 nm, as measured by DLS. It is well

known that the size of the colloids can be adjusted by the amount of surfactant in the system,[39,40] but in the case of NCs, great care has to be taken in order not to induce acorn-like or hemispherical morphologies. The absence of these morphologies can be ensured by limiting the amount of surfactant in the emulsions to avoid the stabilization of the hexadecane/aqueous interface.[40] The TEM micrographs evidenced the core−shell structure of the NCs (Figure 1c, d); in the SEM pictures some capsules appeared to be collapsed under the preparation or the observation conditions. The NCs were found to display a patchy structure (see Figure 1c−f and Figure S1 for NPs) that could be clearly detected by transmission electron microscopy. The presence of nanopatches is verified by the SEM micrographs, which revealed the presence of heterogeneities on the nanoscale on the NCs surface (Figure 1e, f). No treatment with metal oxide vapors was needed here due to the inherent contrast between the PMMA and the PVFc phases caused by the presence of iron in the latter phase (darker phase). The patches (25 ± 3 nm) originated from the microphase separation between the PVFc and PMMA building blocks in the polymer shell. Similar structures in NPs have been obtained for weakly phase-separating polystyrene-*b*-poly(methyl methacrylate),[40] polystyrene-*b*-poly(4-vinylpyridine) block copolymers,[41,42] blends of polystyrene-*b*-polybutadiene with polystyrene,[43] and polystyrene-*b*-poly(ferrocenylethylmethylsilane) block copolymers,[44] but in monolithic NPs. Remarkably, in our case functional patches of PVFc were created in the shell of the NCs, which is an unprecedented case of patchy colloids.

XPS measurements were employed to verify that the vinylferrocene moieties remained stable upon preparation of the NCs. As the amount of iron in NCs is rather low, only signals with very low intensities appeared in the survey spectrum (Figure S2). The XPS measurements of the Fe2p photoelectron emissions were hence performed for ~24 h. The shape of the Fe2p area (Figure 2) indicated the presence of ferrocene (Fe^{II} at 707.5 eV) and a weak signal for ferricenium (Fe^{III} at 710.5 eV).[45,46] The ferricenium in the capsules probably appeared during the measurement. Because of the presence of ferrocene units in the functional nanopatches, the nanocapsules are promising support for oxidation reactions.

Selective Oxidation of the PVFc Nanopatches. It is well known that PVFc can be oxidized by a variety of oxidants.[47,48] We used H_2O_2 and $KMnO_4$ as oxidants because they are water-soluble and they did not influence the colloidal stability of the dispersions. $KMnO_4$ offers the additional advantage of allowing visual monitoring of the reaction by the control of the color. Indeed, the color of the dispersion changed from purple to brown in the first hour. After oxidation, the average hydrodynamic diameter of the NCs

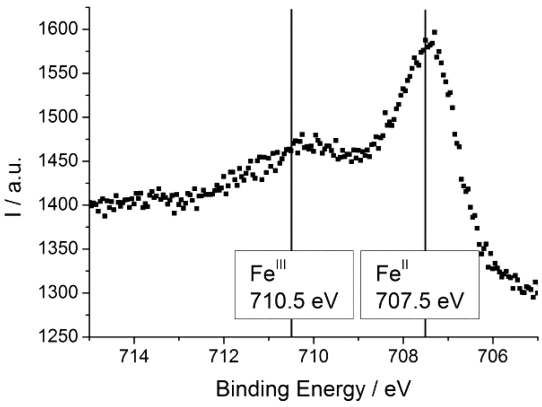

Figure 2. Fe2p area in the XPS spectrum of the NCs.

measured by DLS increased from 236 to 310 nm when treated with H_2O_2, and to 282 upon oxidation with $KMnO_4$ (also see Figure S3a). We attributed the increase of the hydrodynamic diameter to the oxidation reaction: upon oxidation, the PVFc domains are converted to poly(vinylferrocenium) domains that are hydrophilic and therefore swollen in water. HPLC was employed to follow the change of polarity of the block copolymer upon oxidation. A shift to lower elution volume was observed after oxidation of the nanocapsules (Figure S3b) and can be attributed to the higher polarity of the copolymer with ferrocenium units compared to the original copolymer. As expected, the shift is irrespective of the oxidant. In parallel, significant structural changes appeared on the surface of the NCs after the oxidation (Figure 3 and Figure S4 for NPs). In order to verify that the structural changes are not introduced by the vacuum of the scanning electron microscope or by drying effects, SFM experiments[49] under atmospheric conditions (50% humidity, room temperature) were performed (Figure 3 and Figure S5). Whereas the untreated NCs displayed only weak surface irregularities with length scales comparable to the size of the block copolymer domains, the surfaces of the capsules oxidized with H_2O_2 displayed indentations <10 nm in depth after oxidation (Figure 3b). Both size and distances between the indents corresponded to the size and distance between the PVFc domains observed before oxidation. When the NCs were oxidized with $KMnO_4$, there were no holes but patches presenting outgrowths 10−20 nm in height on the surface (Figure 3c). The distribution of size of such outgrown patches was broader than the distribution of size of the indents, as were the distances between them, but it still compared fairly well with the size and distances between the initial nonoxidized PVFc domains.

The proposed mechanisms to explain the structural difference of the patches after oxidation depend on the ability of the oxidant to diffuse in the shell. Upon oxidation, the poly(vinylferrocenium) domains swelled more or less, depending on the oxidant used. Due to

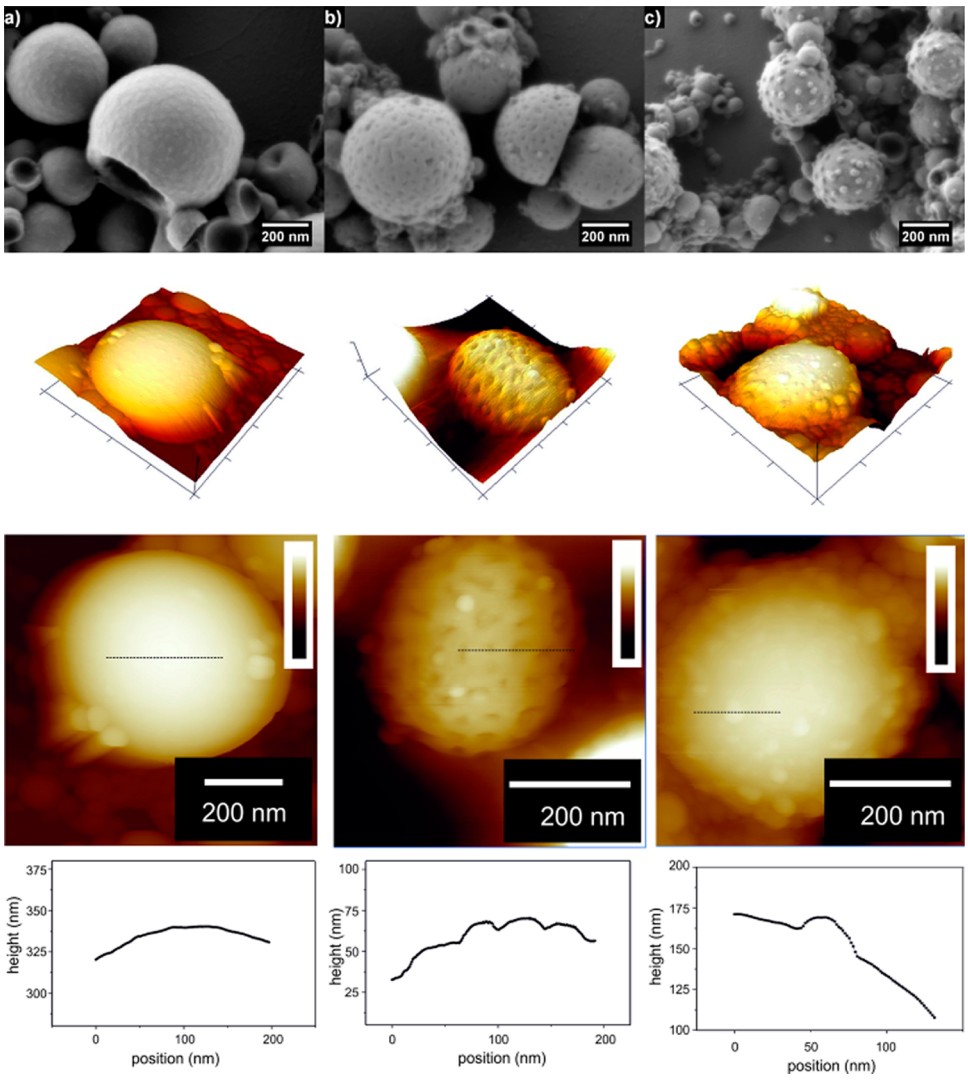

Figure 3. The surface morphology of dialyzed PVFc-*b*-PMMA NCs changes from slightly rough before oxidation (a) to surfaces presenting indents (b) or outgrowths (c) after oxidation with H_2O_2 or $KMnO_4$, respectively. For clarity we have displayed the SFM height images twice: first row in 3D perspective view with back-light illumination and in the second row as standard color-scale images. The *z*-scale bar is 750 nm (untreated), 200 nm (H_2O_2 treated), and 500 nm ($KMnO_4$ treated), respectively. In these images we have indicated with a black dotted line the topography profiles, which are presented in the bottom row. The untreated sample shows a much smoother surface compared to the oxidated NCs. From such profiles we have determined the range of the depths of the indents and the outgrowths.

its ionic character, MnO_4^- is expected to diffuse less rapidly than H_2O_2 in the shell. The poly(vinylferrocenium) is therefore mainly created on the surface, and because the polyvinylferrocene that is buried in the patches cannot react anymore, the poly(vinylferrocenium) chains swell in water, pushing the polymer shell outward. The volume is only locally extended, and outgrowths are observed after drying the sample. On the contrary, H_2O_2 diffuses faster in the shell, thus allowing a spatial rearrangement of the poly(vinylferrocenium) chains. Because a spherical shape is thermodynamically favored compared to the formation of outgrowths, the rearrangement of the poly(vinylferrocenium) chains leads to a slight increase of the whole diameter of the NCs. Upon drying, the poly(vinylferrocenium) chains collapse, leaving empty spaces in the previously swollen channels that appear as holes in the SEM micrographs. Second, the MnO_4^- may interact with the poly(vinylferrocenium) domains after the initial oxidation has taken place, preferably oxidizing ferrocene units spatially very close to poly(vinylferrocenium) side groups, and thus enhancing the local charge density. In contrast, H_2O_2 as an unpolar molecule may oxidize the PVFc side groups more evenly, yielding more uniform and less pronounced surface structures. Conversely, the enhanced charge density after oxidation with $KMnO_4$ may result in locally highly swollen poly(vinylferrocenium) domains. Control experiments were performed by synthesizing PVFc-*b*-PMMA monolithic NPs instead of NCs. The NPs showed similar changes of their morphology upon oxidation (Figure S4), indicating no significant

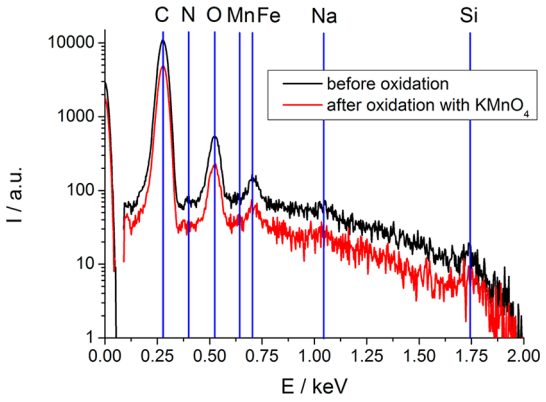

Figure 4. SEM-EDX spectra of a single dialyzed NC before and after oxidation with $KMnO_4$. There are no traces of manganese in the spectrum, indicating that the observed outgrowths are not due to deposited MnO_2.

differences in the oxidation ability of the two morphologies. The counterion dependence of the morphology and volume of poly(ferrocenyldimethylsilane) thin films upon oxidation was also reported.[50] The mechanisms that explain the differences of morphologies of the NCs surface are schematized in Figure S6. To further verify the proposed mechanism for the occurrence of outgrowths and indents, we also used $FeCl_3$ as oxidant. As expected, outgrowths but no indents were detected by SEM (Figure S7) and SFM (Figure S8), as in the case of the oxidation with $KMnO_4$.

Since MnO_2 is produced by the oxidation reaction with $KMnO_4$, it was necessary to verify also that the metal oxide was not present in the outgrowths. The surface composition of NCs was analyzed with SEM-EDX (Figure 4). No peaks for manganese could be detected even when various voltages were applied, and the spectra of the materials before and after oxidation were very similar. Not only is MnO_2 not present in the outgrowths of the NCs oxidized with $KMnO_4$, but the metal oxide was removed during the dialysis.

Finally, reference samples with NCs and NPs of PMMA homopolymer were prepared by the same procedure to verify the stability of PMMA against oxidation. No increase in hydrodynamic diameter was observed for the PMMA colloids after oxidation (see Figure S9). Furthermore, SEM micrographs showed no changes of the morphology on NPs or NCs (Figures S10, S11). Therefore, the observed changes in the PVFc-*b*-PMMA NCs are not due to a partial oxidation or degradation of the PMMA matrix. They occurred solely by the conversion of the ferrocene moiety to ferrocenium moiety upon oxidation and the resulting change in polarity of the polymer. The hydrophobic to hydrophilic transition of the patches upon oxidation represents a promising strategy to fabricate hydrophilic patches on a hydrophobic colloid surface.

To investigate the reversibility of the transition, the NPs and NCs were reduced by the addition of ascorbic acid after being oxidized by H_2O_2, $KMnO_4$, and $FeCl_3$. The color of the dispersions changed back to their original states—from brown to orange with $KMnO_4$ and from slightly greenish to orange with $FeCl_3$—indicating that reduction has taken place at least to some extent. However, no significant changes in the diameter or in the morphology of the NCs or NPs could be detected after the reduction with ascorbic acid, as shown by SEM micrographs (Figure S12). The observations were confirmed by cyclic voltammetry measurements. Indeed, the asymmetric shape of the curves (Figure S13) indicated that the oxidation of the poly(vinylferrocene) block was possible, but the reduction was partially hindered. Thus, the oxidized ferrocene moieties in a dense confinement could not be fully reduced again. After several cycles the signal intensity decreased due to better solubility of the poly(vinylferrocenium) block copolymer in acetonitrile and the formation of a film on the electrode surface. As for the chemical reduction of the oxidized patches, the cyclic voltammetry measurements showed a certain reversibility of the oxidation process.

Redox-Responsive Release of Pyrene. As demonstrated before, accessible responsive patches are present in the nanocapsule shells. This unique feature could be advantageously used to release a molecule present in the core of the NCs upon an oxidation stimulus. Pyrene was chosen as a model for a hydrophobic substance since it is commonly employed as a fluorophore to monitor the release kinetics from compartmentalized objects.[51] Owing to the scattering of light by the colloids and due to partially overlapping absorption bands, the colloids were mixed with a solvent used to partially extract the pyrene released after oxidation. Cyclohexane was chosen because it is a good solvent for pyrene, has no significant influence on the morphology of the polymer shell, and is immiscible with the emulsion, thus allowing a fast separation. This method is milder than centrifugation, which can damage the NCs, thereby artificially increasing the amount of released pyrene. Samples were withdrawn from the reaction mixture at certain intervals of time, with the oxidation reagent added at $t = 0$ min corresponding to the addition of the oxidant. A significant increase in fluorescence intensity with oxidation time of the NCs with H_2O_2 or $KMnO_4$ was observed (Figure 5a). This is indicative of a release of pyrene from the NCs, compared to the almost constant intensity detected for the nonoxidized sample. The nonabsence of fluorescence signal for the untreated sample is due to pyrene absorbed on the surface of the NCs and/or to slow leaking from the NCs. However, the stimuli-responsive behavior of the release is evidenced by the large increase of intensity upon addition of the oxidants, as schematized in Figure 5b. The release upon oxidation with H_2O_2 is far more significant than the release upon oxidation with $KMnO_4$. This is related to

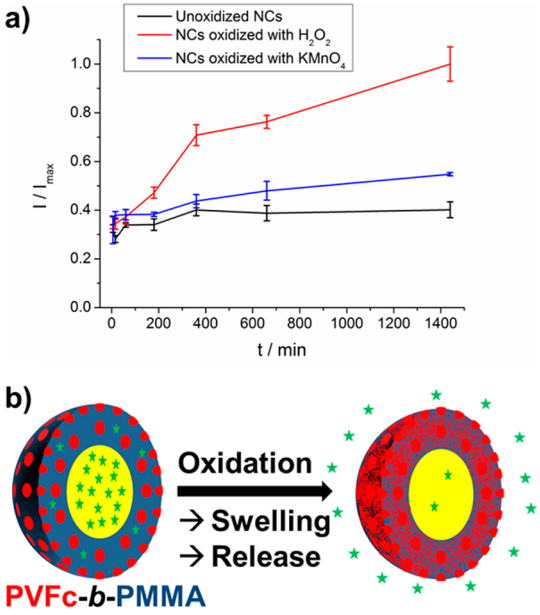

Figure 5. Release kinetics of pyrene from PVFc-*b*-PMMA patchy NCs (a). The fluorescence intensity of the oxidized NCs increases with time, indicating a release of pyrene, whereas the intensity of the nonoxidized NCs remained almost constant. Schematics showing the oxidation-responsive release of the hydrophobic payload from the PVFc-*b*-PMMA patchy NCs (b).

the aforementioned remarks about the different diffusion of the oxidants and hence different loci of oxidation. A larger number of ferrocene units converted to ferrocenium (H_2O_2) allows an enhanced diffusion of pyrene outside the NCs, whereas a more local oxidation ($KMnO_4$) causes a less pronounced release of pyrene. Control experiments performed with NPs instead of NCs showed the same tendency (Figure S14), although the overall release was much lower. Thus, the results indicated a morphology-, time-, and oxidant-dependent release of pyrene from the patchy nanocapsules. H_2O_2 was found to be a more useful oxidizing agent than $KMnO_4$ for the NCs for the release of pyrene.

CONCLUSIONS

Patchy nanocapsules with functional block copolymers as shell were prepared from droplet templates of aqueous emulsions. The nanopatches were composed of poly(vinylferrocene) blocks distributed in the PMMA matrix, and their creation was the result of a microphase separation between both polymer blocks. The poly(vinylferrocene) nanopatches could be selectively oxidized, thereby inducing a transition from a purely hydrophobic patchy object to a hydrophobic object with swollen hydrophilic nanopatches. The topography of the nanocapsules surface after oxidation was dependent on the nature of the oxidizing agent. The hydrophobic to hydrophilic transition of the poly(vinylferrocene) nanopatches was advantageously utilized to release a hydrophobic payload upon selective oxidation of the nanopatches.

The reported synthetic procedure represents a unique strategy to prepare functional patchy nanoobjects. Various functional block copolymer could also be employed to target other types of stimuli-responsive release.

Driven by the early concept of multicompartment polymer micelles envisioned by Ringsdorf,[52] the self-assembly of multicompartment objects is currently the object of intensive research because of the possibility to create unprecedented structures.[53−56] In this respect, our hydrophobic nanoobjects with hydrophilic patches are also promising building blocks for the self-assembly of patchy structures.

EXPERIMENTAL SECTION

Materials. The block copolymer PVFc-*b*-MMA was prepared by living anionic polymerization as described previously.[30] The molecular weight of PVFc was determined *via* SEC against PVFc standards and SEC-MALLS ($M_n \approx 9600$ g·mol^{-1}, $M_w \approx 11\,000$ g·mol^{-1}, PDI = 1.14). The molecular weight of the PVFc-*b*-PMMA was measured *via* SEC in THF against PS standards ($M_n \approx 139\,700$ g·mol^{-1}, $M_w \approx 142\,500$ g·mol^{-1}, PDI = 1.02). Poly(methyl methacrylate) (PMMA, Acros, $M_w \approx 88\,000$ g·mol^{-1}, PDI = 2.29), hexadecane (HD, Acros, 99.8%), sodium dodecyl sulfate (SDS, Alfa Aesar, 99%), dichloromethane (Fisher, 99.99%), cyclohexane (VWR, HPLC-grade), $FeCl_3$ (Sigma-Aldrich, 97%), L-(+)-ascorbic acid (ABCR, 99%), H_2O_2 (Sigma-Aldrich, 35 wt % in water), and $KMnO_4$ (Sigma-Aldrich, 99%) were used as received. Distilled water was used throughout the work.

Preparation of the NPs and NCs. To prepare the NPs, 100 mg of the polymer PVFc-*b*-PMMA or PMMA was dissolved in 2.5 g of CH_2Cl_2. Then a solution of 2 mg of SDS in 20 g of water was added. The mixture was stirred at 1250 rpm in a closed glass vial to obtain a macroemulsion. The emulsion was then subjected to ultrasonication under ice-cooling for 2 min in a pulse−pause regimen of 30 and 10 s, respectively (Branson W450-D sonifier with a 1/2 in. tip). Afterward, the CH_2Cl_2 was evaporated at 40 °C while stirring at 500 rpm overnight. For the preparation of NCs, 60 mg of polymer and 40 mg of hexadecane were dissolved in CH_2Cl_2, and the aforementioned procedure was followed.

Oxidation of the NPs and NCs. For oxidation experiments, the dispersions were diluted to reach a total volume of 24 mL. The diluted dispersions were then divided in three equal parts, which were further treated either with 1 mL of 35% H_2O_2 solution, 1 mL of a freshly prepared $KMnO_4$ solution (158 mg $KMnO_4$ in 100 mL water), 1 mL of 0.0053 mol·L^{-1} $FeCl_3$ aqueous solution, or 1 mL of distilled water. The oxidants were in slight molar excess compared to the VFc units in the copolymer. For NCs, the volume of added solutions of oxidants was reduced to 0.6 mL or to 0.4 mL in the case of pure water to keep the reaction ratio constant. Afterward, the sealed dispersions were stirred for 24 h and dialyzed against distilled water for 48 h with a Visking 27/32 dialysis tube (Roth, cutoff of 14 000 g·mol^{-1}). The NPs and NCs oxidized by H_2O_2 and $KMnO_4$ were reduced by the addition of 0.5 mL of a 0.1 mol·L^{-1} solution of ascorbic acid and stirred for 24 h at room temperature.

Release Experiments. For the release experiments, a solution of 1 mg pyrene in 2.5 g of CH_2Cl_2 was used to dissolve the polymer. After the preparation of the NCs or NPs, the dispersions were dialyzed as described above and treated with the

different oxidizing reagents. A 0.75 mL portion of the dispersion was withdrawn from the vial at certain time intervals. Then 1.5 mL of cyclohexane was added, and the mixture shaken for a short time. After rapid phase separation, 0.75 mL of the upper phase was removed and 0.75 mL of cyclohexane was added again. After shaking and phase separation, the upper phase was removed again. The procedure was repeated one more time; therefore the total volume of cyclohexane amounted to 2.25 mL, from which the fluorescence intensity was measured.

Analytical Tools. The prepared NPs and NCs were characterized with DLS, SEC, HPLC, SFM, XPS, cyclic voltammetry, and electron microscopy, while fluorescence analysis was used to measure the release of pyrene (see Supporting Information).

Conflict of Interest: The authors declare no competing financial interest.

Acknowledgment. We thank Helma Burg and Uwe Rietzler, Gennady Cherkashinin, Gunnar Glasser, and Beate Müller for AFM, XPS, SEM-EDX, and HPLC measurements, respectively. Support in performing the SEC analyses by Marion Trautmann is acknowledged. M.G. thanks the Landesoffensive zur Entwicklung Wissenschaftlich-ökonomischer Exzellenz (LOEWE Soft Control) for financial support of this work. R.H.S. gratefully acknowledges a scholarship from the Fonds der Chemischen Industrie (FCI).

Supporting Information Available: Additional images, data, and detailed descriptions of characterization methods are supplied. This material is available free of charge *via* the Internet at http://pubs.acs.org.

REFERENCES AND NOTES

1. Page, C. C.; Moser, C. C.; Chen, X.; Dutton, P. L. Natural Engineering Principles of Electron Tunnelling in Biological Oxidation-Reduction. *Nature* **1999**, *402*, 47–52.
2. Dröge, W. Free Radicals in the Physiological Control of Cell Function. *Physiol. Rev.* **2002**, *82*, 47–95.
3. Stamler, J. S. Redox Signaling: Nitrosylation and Related Target Interactions of Nitric Oxide. *Cell* **1994**, *78*, 931–936.
4. Coyle, J. T.; Puttfarcken, P. Oxidative Stress, Glutamate, and Neurodegenerative Disorders. *Science* **1993**, *262*, 689–695.
5. Finkel, T.; Holbrook, N. J. Oxidants, Oxidative Stress and the Biology of Ageing. *Nature* **2000**, *408*, 239–247.
6. Liu, R.; Zhao, X.; Wu, T.; Feng, P. Tunable Redox-Responsive Hybrid Nanogated Ensembles. *J. Am. Chem. Soc.* **2008**, *130*, 14418–14419.
7. Wan, X.; Wang, D.; Liu, S. Fluorescent pH-Sensing Organic/Inorganic Hybrid Mesoporous Silica Nanoparticles with Tunable Redox-Responsive Release Capability. *Langmuir* **2010**, *26*, 15574–15579.
8. Bird, R.; Freemont, T. J.; Saunders, B. R. Hollow Polymer Particles That Are pH-Responsive and Redox Sensitive: Two Simple Steps to Triggered Particle Swelling, Gelation and Disassembly. *Chem. Commun.* **2011**, *47*, 1443–1445.
9. Goldenbogen, B.; Brodersen, N.; Gramatica, A.; Loew, M.; Liebscher, J.; Herrmann, A.; Egger, H.; Budde, B.; Arbuzova, A. Reduction-Sensitive Liposomes from a Multifunctional Lipid Conjugate and Natural Phospholipids: Reduction and Release Kinetics and Cellular Uptake. *Langmuir* **2011**, *27*, 10820–10829.
10. Ong, W.; Yang, Y.; Cruciano, A. C.; McCarley, R. L. Redox-Triggered Contents Release from Liposomes. *J. Am. Chem. Soc.* **2008**, *130*, 14739–14744.
11. Wang, C.; Guo, Y.; Wang, Y.; Xu, H.; Zhang, X. Redox Responsive Supramolecular Amphiphiles Based on Reversible Charge Transfer Interactions. *Chem. Commun.* **2009**, 5380–5382.
12. Napoli, A.; Valentini, M.; Tirelli, N.; Muller, M.; Hubbell, J. A. Oxidation-Responsive Polymeric Vesicles. *Nat. Mater.* **2004**, *3*, 183–189.
13. Tatsuma, T.; Saito, K.; Oyama, N. Enzyme Electrodes Mediated by a Thermoshrinking Redox Polymer. *Anal. Chem.* **1994**, *66*, 1002–1006.
14. Saito, T.; Watanabe, M. Characterization of Poly-(vinylferrocene-co-2-Hydroxyethyl Methacrylate) for Use As Electron Mediator in Enzymatic Glucose Sensor. *React. Funct. Polym.* **1998**, *37*, 263–269.
15. Saito, T.; Watanabe, M. Electron Transfer Reaction from Glucose Oxidase to an Electrode *via* Redox Copolymers. *Polym. J.* **1999**, *31*, 1149–1154.
16. Patel, H.; Li, X.; Karan, H. I. Amperometric Glucose Sensors Based on Ferrocene Containing Polymeric Electron Transfer Systems - A Preliminary Report. *Biosens. Bioelectron.* **2003**, *18*, 1073–1076.
17. Gülce, A.; Gülce, H. Polyvinylferrocenium Modified Pt Electrode for Anaerobic Glucose Monitoring. *J. Biochem. Biophys. Methods* **2005**, *62*, 81–92.
18. Cass, A. E. G.; Davis, G.; Francis, G. D.; Hill, H. A. O.; Aston, W. J.; Higgins, I. J.; Plotkin, E. V.; Scott, L. D. L.; Turner, A. P. F. Ferrocene-Mediated Enzyme Electrode for Amperometric Determination of Glucose. *Anal. Chem.* **1984**, *56*, 667–671.
19. Nakahata, M.; Takashima, Y.; Yamaguchi, H.; Harada, A. Redox-Responsive Self-Healing Materials Formed from Host-Guest Polymers. *Nat. Commun.* **2011**, *2*, 511.
20. Whittell, G. R.; Manners, I. Metallopolymers: New Multifunctional Materials. *Adv. Mater.* **2007**, *19*, 3439–3468.
21. Abd-El-Aziz, A. S.; Manners, I. *Frontiers in Transition Metal-Containing Polymers*; Wiley-Interscience: Hoboken, NJ, 1997.
22. Manners, I. *Synthetic Metal-Containing Polymers*; VCH: Weinheim, Germany, 2004.
23. Wöhrle, D.; Pomogailo, A. D. *Metal Complexes and Metals in Macromolecules: Synthesis, Structure and Properties*; Wiley-VCH: Weinheim, Germany, 2003.
24. Carraher, C. E.; Abd-El-Aziz, A. S.; Pittman, C.; Sheats, J.; Zeldin, M. *A Half Century of Metal and Metalloid Containing Polymers*; Wiley: New York, 2003.
25. Rehahn, M. Organic-Inorganic Hybrid Polymers. In *Synthesis of Polymers*; Wiley-VCH: Weinheim, Germany, 1999.
26. Smith, T. M.; Nelson, G. L. Ferrocene Containing Copolymers with Improved Electrostatic Dissipation Properties for Advanced Applications. *Polym. Adv. Technol.* **2006**, *17*, 746–753.
27. Foucher, D. A.; Tang, B. Z.; Manners, I. Ring-Opening Polymerization of Strained, Ring-Tilted Ferrocenophanes: a Route to High-Molecular-Weight Poly(ferrocenylsilanes). *J. Am. Chem. Soc.* **1992**, *114*, 6246–6248.
28. Manners, I. Ring-Opening Polymerization (ROP) of Strained Metallocenophanes: The Discovery and Development of a New Route to High Molecular Weight Poly(metallocenes). *Can. J. Chem.* **1998**, *76*, 371–381.
29. Bellas, V.; Rehahn, M. Polyferrocenylsilane-Based Polymer Systems. *Angew. Chem., Int. Ed.* **2007**, *46*, 5082–5104.
30. Gallei, M.; Klein, R.; Rehahn, M. Silacyclobutane-Mediated Re-Activation of "Sleeping" Polyvinylferrocene Macro-Anions: A Powerful Access to Novel Metalloblock Copolymers. *Macromolecules* **2010**, *43*, 1844–1854.
31. Gallei, M.; Schmidt, B. V. K. J.; Klein, R.; Rehahn, M. Defined Poly[styrene-block-(ferrocenylmethyl methacrylate)] Diblock Copolymers *via* Living Anionic Polymerization. *Macromol. Rapid Commun.* **2009**, *30*, 1463–1469.
32. Crespy, D.; Stark, M.; Hoffmann-Richter, C.; Ziener, U.; Landfester, K. Polymeric Nanoreactors for Hydrophilic Reagents Synthesized by Interfacial Polycondensation on Miniemulsion Droplets. *Macromolecules* **2007**, *40*, 3122–3135.
33. Crespy, D.; Staff, R. H.; Becker, T.; Landfester, K. Chemical Routes Toward Multicompartment Colloids. *Macromol. Chem. Phys.* **2012**, *213*, 1183–1189.
34. Fickert, J.; Rupper, P.; Graf, R.; Landfester, K.; Crespy, D. Design and characterization of Functionalized Silica Nanocontainers for Self-Healing Materials. *J. Mater. Chem.* **2012**, *22*, 2286–2291.
35. Crespy, D.; Landfester, K. Miniemulsion Polymerization As a Versatile Tool for the Synthesis of Functionalized Polymers. *Beilstein J. Org. Chem.* **2010**, *6*, 1132–1148.
36. Texter, J. Precipitation and Condensation of Organic Particles. *J. Dispersion Sci. Technol.* **2001**, *22*, 499–527.

37. Landfester, K.; Montenegro, R.; Scherf, U.; Güntner, R.; Asawapirom, U.; Patil, S.; Neher, D.; Kietzke, T. Semiconducting Polymer Nanospheres in Aqueous Dispersion Prepared by a Miniemulsion Process. *Adv. Mater.* **2002**, *14*, 651–655.
38. Crespy, D.; Landfester, K. Preparation of Nylon 6 Nanoparticles and Nanocapsules by Two Novel Miniemulsion/Solvent Displacement Hybrid Techniques. *Macromol. Chem. Phys.* **2007**, *208*, 457–466.
39. Staff, R. H.; Lieberwirth, I.; Landfester, K.; Crespy, D. Preparation and Characterization of Anisotropic Submicron Particles from Semicrystalline Polymers. *Macromol. Chem. Phys.* **2012**, *213*, 351–358.
40. Staff, R. H.; Rupper, P.; Lieberwirth, I.; Landfester, K.; Crespy, D. Phase Behavior of Binary Mixtures of Block Copolymers and a Non-Solvent in Miniemulsion Droplets as Single and Double Nanoconfinement. *Soft Matter* **2011**, *7*, 10219–10226.
41. Kim, M. P.; Kang, D. J.; Jung, D.-W.; Kannan, A. G.; Kim, K.-H.; Ku, K. H.; Jang, S. G.; Chae, W.-S.; Yi, G.-R.; Kim, B. J. Gold-Decorated Block Copolymer Microspheres with Controlled Surface Nanostructures. *ACS Nano* **2012**, *6*, 2750–2757.
42. Deng, R.; Liu, S.; Li, J.; Liao, Y.; Tao, J.; Zhu, J. Mesoporous Block Copolymer Nanoparticles with Tailored Structures by Hydrogen-Bonding-Assisted Self-Assembly. *Adv. Mater.* **2012**, *24*, 1889–1893.
43. Jeon, S.-J.; Yi, G.-R.; Yang, S.-M. Cooperative Assembly of Block Copolymers with Deformable Interfaces: Toward Nanostructured Particles. *Adv. Mater.* **2008**, *20*, 4103–4108.
44. Rider, D. A.; Chen, J. I. L.; Eloi, J.-C.; Arsenault, A. C.; Russell, T. P.; Ozin, G. A.; Manners, I. Controlling the Morphologies of Organometallic Block Copolymers in the 3-Dimensional Spatial Confinement of Colloidal and Inverse Colloidal Crystals. *Macromolecules* **2008**, *41*, 2250–2259.
45. Umana, M.; Rolison, D. R.; Nowak, R.; Daum, P.; Murray, R. W. X-ray Photoelectron Spectroscopy of Metal, Metal Oxide, and Carbon Electrode Surfaces Chemically Modified with Ferrocene and Ferricenium. *Surf. Sci.* **1980**, *101*, 295–309.
46. Han, L. M.; Rajeshwar, K.; Timmons, R. B. Film Chemistry Control and Electrochemical Properties of Pulsed Plasma Polymerized Ferrocene and Vinylferrocene. *Langmuir* **1997**, *13*, 5941–5950.
47. Ritter, H.; Mondrzik, B. E.; Rehahn, M.; Gallei, M. Free Radical Homopolymerization of a Vinylferrocene/Cyclodextrin Complex in Water. *Beilstein J. Org. Chem.* **2010**, *6*, DOI 10.3762/bjoc.6.60.
48. D'Silva, C.; Afeworki, S.; Parri, O. L.; Baker, P. K.; Underhill, A. E. Electrochemical Characterisation of Polyvinylferrocene Polymers: Substituent Effects on the Redox Reaction. *J. Mater. Chem.* **1992**, *2*, 225–230.
49. Butt, H.-J.; Berger, R.; Bonaccurso, E.; Chen, Y.; Wang, J. Impact of Atomic Force Microscopy on Interface and Colloid Science. *Adv. Colloid Interface Sci.* **2007**, *133*, 91–104.
50. Péter, M.; Hempenius, M. A.; Kooij, E. S.; Jenkins, T. A.; Roser, S. J.; Knoll, W.; Vancso, G. J. Electrochemically Induced Morphology and Volume Changes in Surface-Grafted Poly(ferrocenyldimethylsilane) Monolayers. *Langmuir* **2004**, *20*, 891–897.
51. Schatz, C.; Smith, E. G.; Armes, S. P.; Wanless, E. J. Reversible pH-Triggered Encapsulation and Release of Pyrene by Adsorbed Block Copolymer Micelles. *Langmuir* **2008**, *24*, 8325–8331.
52. Ringsdorf, H.; Lehmann, P.; Weberskirch, R. *Multicompartmentation—a Concept for the Molecular Architecture of Life*; 217th ACS National Meeting, Anaheim, CA, **1999**.
53. Li, Z.; Kesselman, E.; Talmon, Y.; Hillmyer, M. A.; Lodge, T. P. Multicompartment Micelles from ABC Miktoarm Stars in Water. *Science* **2004**, *306*, 98–101.
54. Cui, H.; Chen, Z.; Zhong, S.; Wooley, K. L.; Pochan, D. J. Block Copolymer Assembly *via* Kinetic Control. *Science* **2007**, *317*, 647–650.
55. Attia, A. B. E.; Ong, Z. Y.; Hedrick, J. L.; Lee, P. P.; Ee, P. L. R.; Hammond, P. T.; Yang, Y.-Y. Mixed Micelles Self-Assembled from Block Copolymers for Drug Delivery. *Curr. Opin. Colloid Interface Sci.* **2011**, *16*, 182–194.
56. Gröschel, A. H.; Schacher, F. H.; Schmalz, H.; Borisov, O. V.; Zhulina, E. B.; Walther, A.; Müller, A. H. E. Precise Hierarchical Self-Assembly of Multicompartment Micelles. *Nat. Commun.* **2012**, *3*, 710.